Soft Matter

Freestanding organogels by molecular velcro of unsaturated amphiphiles

Journal:	*Soft Matter*
Manuscript ID	SM-ART-02-2019-000378.R2
Article Type:	Paper
Date Submitted by the Author:	10-Jun-2019
Complete List of Authors:	Balachandran, Vijai Shankar; the City College of New York, Chemistry Kizhmuri, Divya; City College Of New York, Department of Chemistry Samateh, Malick; City College Of New York, Department of Chemistry Sagiri, Sateesh; City College Of New York, Department of Chemistry Satapathy, Sitakanta; City College Of New York, Department of Chemistry Pradhan, Padmanava; City College Of New York, Department of Chemistry Raghavan, Srinivasa; University of Maryland, Chemical and Biomolecular Engineering Rakesh, Leela; CMU, Math Sellers, Michael; Army Research Laboratory Karna, Shashi; U.S. Army Research Laboratory John, George; City College Of New York, Department of Chemistry

Soft Matter

RSCPublishing

FULL PAPER

Freestanding organogels by molecular velcro of unsaturated amphiphiles

Cite this: DOI: 10.1039/x0xx00000x

Received ooth January 20xx,
Accepted ooth January 20xx

DOI: 10.1039/x0xx00000x

www.rsc.org/

Vijai Shankar Balachandran,[a¶§] Kizhmuri P. Divya,[a¶] Malick Samateh,[a,b] Sai S. Sagiri,[a] Sitakanta Satapathy, [a]Padmanava Pradhan, [a]Srinivasa R. Raghavan, [c] Leela Rakesh,[d]* Michael S. Sellers,[e] Shashi P. Karna,[e]* and George John[a,b]*

A simple amphiphile, N-cardanyltaurine amide (NCT) with different degrees of *cis*-unsaturation in its tail resulted in forming strong organogels. Interestingly, this is in contrast to the commonly accepted notion that introducing unsaturation in alkyl chains enhances fluidity in lipid assemblies. Physico-chemical and first principles DFTcalculations confirmed the pegging of 'kinked' unsaturated side chains, where the hydrophobic interlocking as in Velcro fasteners leads to a network of cylindrical micelles, resulting in self-standing organogels. Textural profile analysis and spectroscopic details substantiated the dynamic assembly to resemble a 3D network of gelators rather than being a cross-linked or polymerized matrix of monomers.

Introduction

Materials from nature such as bone, skin, nacre and wood etc. exhibit multiple levels of hierarchical structures at the nano and microscales, to impart intricate functionality.[1,2] Such multilevel hierarchy has been replicated in biomimetic materials that exhibit adhesion to dry surfaces or super hydrophobicity.[3,4] Exploring the fundamental interactions in natural systems has enhanced our understanding at the molecular level and provided clues to replicate the same in generating new functional materials.[5] One such interesting phenomenon is the interlocking of hook-like structures, widely observed in nature. The adhesion of cocklebur (*Xanthium strumarium*) seeds, Velcro®, colonies of *Aztecaandrae* ants[6,7] are some of the examples where hooking plays an important role in their survival. Nanoscale structures with hooked morphology has shown mechanical interlocking to exhibit adhesion and resilience property.[8,9] Observation of these interesting systems for such fascinating phenomena has motivated us to explore whether such interlocking can be mimicked via molecular interactions for bioinspired self-assembled materials.

One thrust area of our research is on the synthesis and assembly of unsaturated amphiphilic molecular systems.[10] Molecular kinks in lipid tails ascribed to –C=C– *cis*-unsaturations[11] are known to be a key factor in dictating the packing of lipids in cell membranes.[12,13] and imperative for fluidity.[14,15] It is demonstrated that kinks in lipids arising from *cis*- double bonds could dictate the assembly of interlocked bilayers.[16] Herein, we report formation of molecular gels, from a simple amphiphile; N-cardanyltaurine amide (NCT)[11] (Fig. 1a) that possess *cis*-unsaturations in its tail. NCT forms reverse assemblies in organic solvents to form self-standing organogels with enhanced yield strength compared to that of their saturated counterpart. As shown in Fig. 1, organogels of NCT in diesel or toluene (2.0 wt%) are freestanding and moldable.

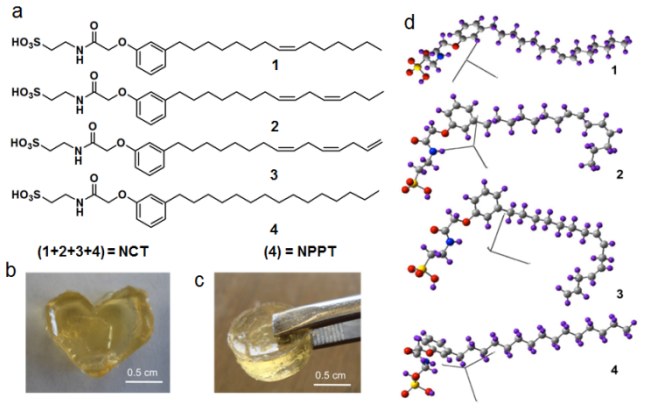

Fig. 1a) Molecular structures of N-Cardanyltaurine amide (NCT) and N-pentadecylphenyltaurine amide (NPPT); b) NCT (2.0 wt%) gel in diesel; c) NCT (2.0 wt%) gel in toluene; d) optimized structures (B3LYP/6-31-G) with respective Cartesian axes of NCT showing kinked side chains. (Red=O, Grey=C, Blue=N, Yellow=S, Purple= H).

Results and discussion

NCT was synthesized from cardanol, a byproduct of cashew industry. Cardanol is a biobased non-isoprene lipid obtained by thermal treatment of cashew nut shell liquid (CNSL). It consists of a rich mixture of phenolic lipids: 5% of 3-(pentadecyl) phenol, 49% of 3-(8Z-pentadecenyl) phenol, 17% of 3-(8Z,11Z-pentadecadienyl)-phenol and 29% of 3-(8Z,11Z,14-pentadecatrienyl)phenol.[17] Thus NCT exists as a mixture of different types of C_{15} tail with one, two, three, or no *cis*-unsaturations. The molecule with no unsaturation is denoted as N-pentadecylphenyltaurine amide (NPPT). The minimum gelation concentration (MGC) of NCT ranged from 1 to 2 wt%, depending on the solvent (Table S1). In all cases, gelation was found to be thermo-reversible.

Experimental Characterization of NCT Gel

The NCT gels showed that the storage modulus G' was independent of frequency and much higher than the loss modulus G'' over the frequency range (Figure. 2a &S3a). This response is typical of a molecular gel, as it indicates that the sample does not relax over long time scales. The G' value for NCT gel was about 1000 Pa. The value of the dynamic yield stress σ_y is 100 Pa, which is relatively high, and consistent with the freestanding nature of the gel.

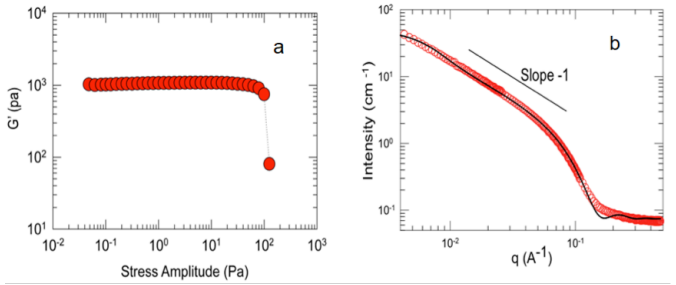

Fig. 2a) Stress sweep dynamic rheology profile of NCT gel showing the yield stress of ~100 Pa, (b) Small Angle Neutron Scattering (SANS) of 2.5 wt% NCT gel in d_8-toluene.

Small-angle neutron scattering (SANS) showed a q^{-1} dependence of the scattering intensity at low q, suggesting the presence of cylindrical assemblies in the organogels (Fig. 2b). The formation of such reverse micellar self-assemblies are fascinating and unfortunately, the reports on such systems have been rarely investigated in other mediums except water.[18-25] Guinier plot (ln [Iq] vs [q^2]) yielded an estimate of the chain diameter to be ~4.6 nm which is in line with twice the average length of an NCT molecule. The end-to-end length of the chains is expected to be >100 nm and it cannot be accurately estimated from the SANS data because it falls outside the window of length scales probed by SANS. Based on the amphiphilic structure, NCT is expected to form reverse micelles. The formation of reverse micelles was also confirmed by the ability of NCT gels in toluene to entrap polar rhodamine-6G hydrochloride. (Fig. S1a).

TEM analysis of the gel showed smooth spaghetti-like cylindrical structures of ~25 nm in diameter and several micrometers in length. (Fig. 3a) AFM analysis also corroborated similar self-assembled structures in the gels (Fig. 3b). These results suggest that the reverse worm-like cylindrical structures (~5 nm in diameter) are clustered together via hydrophobic unsaturated tails interlocking to form a larger assembly of ~25 nm. SEM images of the xerogel showed stacked sheets of 20-35 nm thick (Fig. 3c, 3d). Such 2D sheets are expected to be formed by the coalescence of the larger assemblies, vide Fig. 3e, facilitated by the reduction in surface tension during phasing out (gelation). Such a mechanism of fusing fibrous bundles in to sheets has been reported in cross-linked actin and myosin systems,[26] and peptide self-assemblies[27] where membranes with curved geometries are formed out of Rayleigh instabilities.[28]The formation of freestanding gel, induced by hydrophobic interlocking of unsaturated alkyl chains is unreported in the literature.

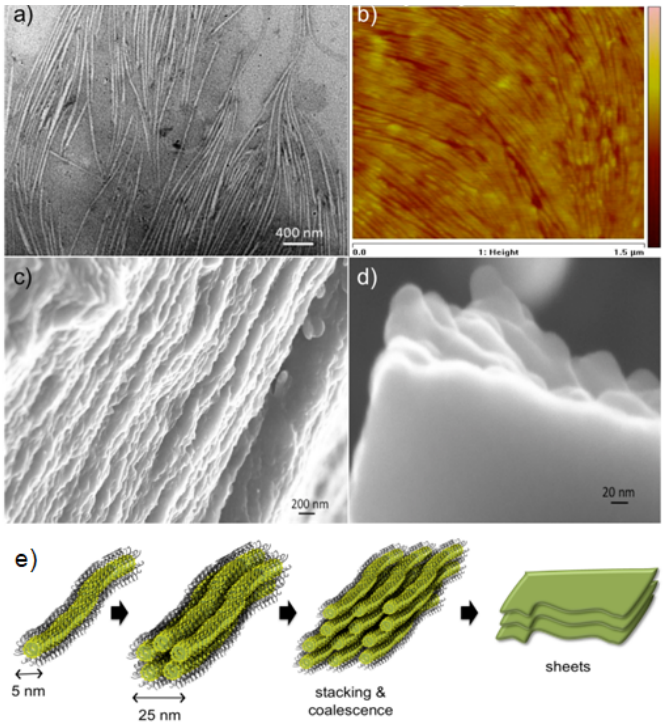

Fig. 3 a) TEM image of a 2.0 wt.% NCT toluene gel; b) AFM image of 2.0 wt.% NCT butanol gel; c) SEM image of 2.0 wt.% toluene gel. d) stacked sheet like morphology at higher magnification; e) schematic of drying induced structure transformation.

Mesoscale modeling and simulation of reverse cylindrical structures.

DPD (Dissipative Particle Dynamics) simulations were used to probe the rationale behind formation of worm like assembly for NCTs in toluene.[29] The mesoscopic course-grain (CG) model (NCTs + Toluene) for simulation under boundary condition was considered to comprise of three beads, where the hydrophilic

and hydrophobic components of NCTs were the head (H) and the tail (T) beads, respectively, while toluene as the solvent was considered to represent a single bead (Simulation details are provided in Computational Section, SI). The simulation results at 313 K revealed the NCT beads in toluene to gradually self-assemble from short (Fig. 4a) to relatively long (Fig 4b) worm-like cylindrical chains as the system approaches to equilibrium state at higher timescales (Fig. S7,S9, SI). The hydrophilic (–SO_3H side) H-beads and the hydrophobic (alkyl chain and phenyl groups) T-beads radially projects in and out respectively, accounting for the reverse miceller assembly, vide Figure 4c. The micellar worm like assembly was consistent for two different NCT:Toluene bead compositions (Fig. S7, S11, SI), validating the AFM and TEM results in Fig 3.

To further investigate the interactions responsible for "pegging" of the kinked hydrophobic chains, molecular dynamics (MD) simulations and first principles density functional (DFT) calculations were performed (Computaional Details, SI). The interacting alkyl chain components of the NCT derivatives were considered exclusively for simulation in order to reduce the computational cost. A sum total of 10 pairs of saturated/unsaturated C_{15} lipid chains ("monoene" + "monoene", "monoene" + "diene", "diene" + "diene" and so on) with the number and location of double bonds similar to those of the NCT amphiphiles were constructed. The respective energies were calculated at the C_1–C_1 separation distances ranging from ~10.0 to ~30.0 Å using NAMD molecular dynamics with the CHARMM36 force field.

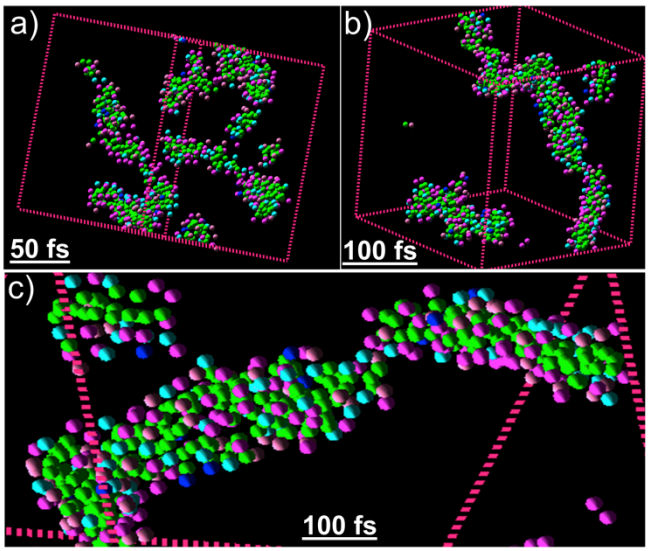

Fig. 4 Snapshots collected from DPD simulation after a) 50 fs and b) 100 fs, depicting shorter and longer worm like micelles, respectively. c) A selected area snapshot after 100 fs accounting for the reverse micellar cylindrical assembly, where the hydrophilic H-beads (Green) and hydrophobic T-beads (other colors) are mostly projected inward and outward, respectively. [Course grain model details: –SO_3H side head bead (H): Green, phenyl + alkyl chain tail bead (T) of D_0 : Pink, D_1 : Blue, D_2 : Sky blue and D_3 : Magenta, where D_n's represent the respective amphiphiles with 'n' accounting for different degrees of *cis*-unsaturation. Toluene beads are excluded for clarity purpose. Time evolution of potential energies along with snapshots collected at different timescales and NCT : toluene compositions are provided in Figures S11, SI].

The interaction energies as a function of distance for all the constructed pairs are shown in Fig. 5 and Table S2. Fig.5 highlights four pairs, i.e., (1) triene" + "triene" (green); (2) "diene" + "diene" (yellow); (3) "monoene" + "triene" (blue); and (4) "saturated" + "saturated" (magenta) of interest. The calculations reveal that the interaction energies are significantly high for the pairs (1) and (2), however relatively low for (3) and (4) over the distances. The pairs (1) to (3) exhibit a moderate amount of interlocking. As expected, pair (4) did not exhibit any interlocking and the saturated alkyl chains remain parallel to one another. These results suggest that chain-chain interlocking could stabilize the pairs of unsaturated chains while compensating for the loss of interaction energy. It is noteworthy to mention that the NCT chains comprise 50% and 29% of "monoene" and "triene", respectively.

From the above studies, we suggest the following mechanism to account for the formation of self-sustainable strong organogels. In non-polar solvents, NCT form reverse cylindrical micelles with the polar –SO_3H group at the core and the alkyl tails projecting outwards into the solvent. These long micellar assemblies entangle through the solvent to form a 3-D network, resulting in gelation. Due to the kinks in its unsaturated tails, an additional type of interaction, i.e., the interlocking of cis-unsaturated chains is also noticed. When two NCT micellar chains approach each other, the kinked alkyl tails on the exterior of each chain peg with respect to each other at the overlapping points (Scheme 1) to form a network. This velcro like interlocking strengthens the junction points in the micellar network and thus account for the significantly high strength of the NCT gels. Interestingly, the long cylindrical micelles of NCT showed an aligning capability of small organic molecules (Fig. S4) such as toluene in the gel state similar to the strain induced alignment (SAG) of $CDCl_3$ in stretched polymeric structures.[30]

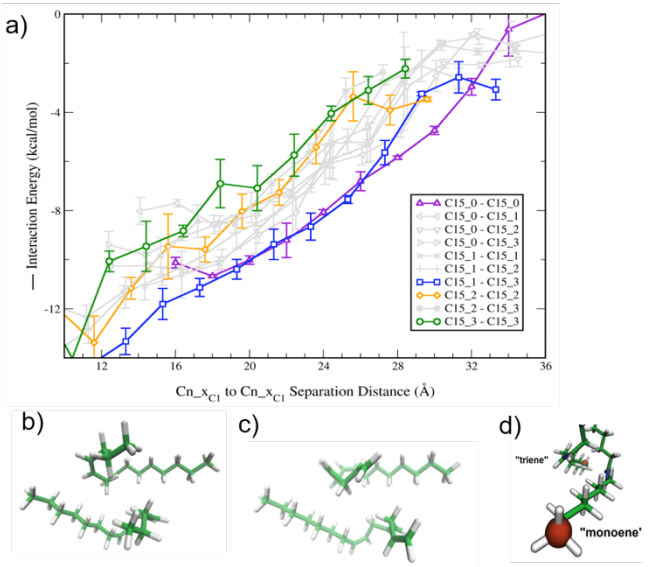

Fig. 5 a) Plot of interaction energy (kcal/mol) with respect to frozen carbon atom **(C1-C1)** separation distance for all ten combinations of saturated/unsaturated

alkyl chains in the NCT mixture. Data sets are labeled as C15_X, where X is the number of double bonds in the alkyl chain. The pairs which resulted in unique structures are highlighted in *green*, *yellow, blue,* and *magenta.* The error bars represent the standard deviation of three independent simulations at each point. Alkyl chain pair configurations at ~18.0 Å after MD simulation; b) "diene"+"diene" c) "triene"+"triene" and d) "monoene"+"triene" pairs. Red spheres identify end locations of frozen carbon atoms and green cylinders identify unsaturated C-C bonds.

Modeling of the Velcro like interlocked cylindrical structures

We propose a model in order to understand the inter-locking mechanism, as shown in Scheme 1. The model consists of two cylindrical filaments of NCT, i.e., C_1 and C_2, with radii r_1 and r_2, interacting along length *l*. The areas of contact of C_1 and C_2 are given by$A_1$and A_2 (shaded grey area, Scheme 1), respectively. A bilayer of molecular leaftlets interacting in a slip-stacked manner through van der Waals and dispersive forces exist in between $A_1$and A_2. The average length of overlap in between the leaflets is D and their interaction is controlled by the molecular density at the respective areas A_1 and A_2, which in turn maximizes the interlocking at the jucntions. The frictional coupling and shear forces in between the leaflets (hemifusion under the bilayer model) are controlled by the extent of interdigitation between them and viscosity of the solvent.[31]Hemifusion depends on the force per unit area and the inter-leaflet frictional coefficient, which is enhanced by the interdigitation between the alkyl chains (leaflets) and thus strengthens the shear force due to the asymmetry created by the short and long alkyl chain lengths.[32] The effective decrease in chain length and *pegging* resulting from the kinks of *cis* double bonds. This enhances the interlocking across *D*, imparting high shear strength to the gel.

In addition to the interlocking, the high shear strength of the gel is further attributed to multiple interactions, e.g., the directional H-bonding between amides and carbonyls and π-π stacking of the aromatic cores. The hydrophobic pegging and the hydrogen bonding are orthogonal with respect to each other,which imparts significantly high shear strength to the gel.

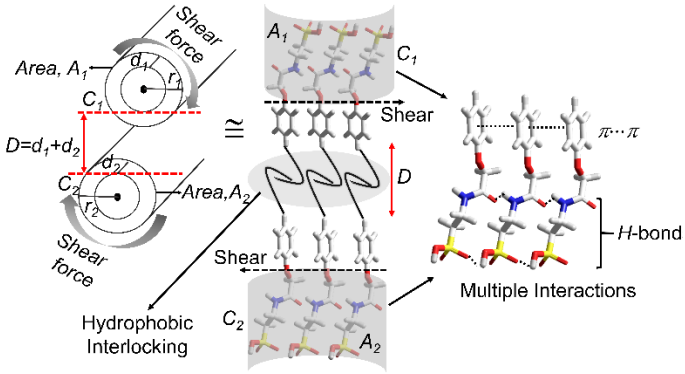

Scheme 1. Schematic showing the geometric models and parameters describing the interactions between the worm-like micelles and the contributing non-covalent forces.

Studies on hydrodynamic forces between brush-like polymers show that, at distances D <*l*/2, the interpenetrating chains behave like 'solid' with increased relaxation time of the chains.[33] Coarse-grain (CG) modeling of polymer brushes with DPD methods show entanglement of chains in solvents of identical polarity resulted in an increase in friction. These models provide useful information on the elasticity and minimum distance for effective interaction. These are based on the classic Flory's polymer brush model, which are extended to lipid bilayers with an inverse cube dependence of surface pressure per alkyl chain. The alkyl chains here are equivalent to the structureless polymer chains with confined solvophobic forces.[34]

Cardanol derived amphiphiles provide interesting self-assembly properties.[11,35] For them to self-assemble in a given solvent medium, (differing in terms of their hydrophilic heads) the hydrophilic counterpart provides significant driving force (H-bond and solute-solvent interactions) governed by the packing factor.[36] Rigid glucoside head groups attached to the cardanol moiety form either helical self-assembles or lipid nanotubes whereas the flexible taurine derived head group in the present case prefer truncated conical structure (the critical packing factor [CPP]<½) leading to cylindrical micellar self-assembly. Further in the present case, the collective hydrophobicity of cardanol moiety with varying *cis* -C=C, provided the appropriate hydrophobicity to form gels. We believe that this results in interlocking/pegging of the incoming NCT amphiphile instead of interdigitated fashion to form bilayers. The repercussion of this phenomenon is also evident from the interaction energies of various *cis* -C=C pairs as given in Figure 5a. This also suggests that the free standing nature of the gel is dependent on the number of such strong "interlocking density" which would be further explored in our future studies. Due to the formation of reverse bilayers by cardanol derivative with glucoside head group, they never formed very strong gels in toluene as in the case of NCT.

If the above mechanism explains the freestanding ability and strength, then removal or absence of kinks in the molecular structure should disfavor the formation of the interlocks and hence the secondary network. Therefore, one would expect a weak molecular non-self-standing gel. To prove this, a fully saturated derivative of NCT, termed as NPPT (Fig. 1) was synthesized as a control molecular system and tested for its gelation behavior. NPPT being an amphiphile, also formed molecular gels, but not free-standing ones (Fig. S2). A 2.0 wt% NPPT gel in toluene had a storage modulus (G') of ~36 Pa (Fig. S2), which is about ~30 times lower than that of a 2.0 wt% NCT gel in toluene (G′ ~1000 Pa). Moreover, the yield stress (σ_y) of the NPPT gel was only ~4.0 Pa (Fig. S2), which is 25 times lower than the σ_y (~100 Pa) of the NCT gel. NPPT gels are paste-like and *not* freestanding or moldable. Polarizing optical microscopic investigations of the NPPT gels showed highly birefringent fibrillar gels, whereas the NCT gels were non-birefringent (Fig. 6). Thus, the absence of unsaturation in the tail of the amphiphile significantly changes the self-assembly.

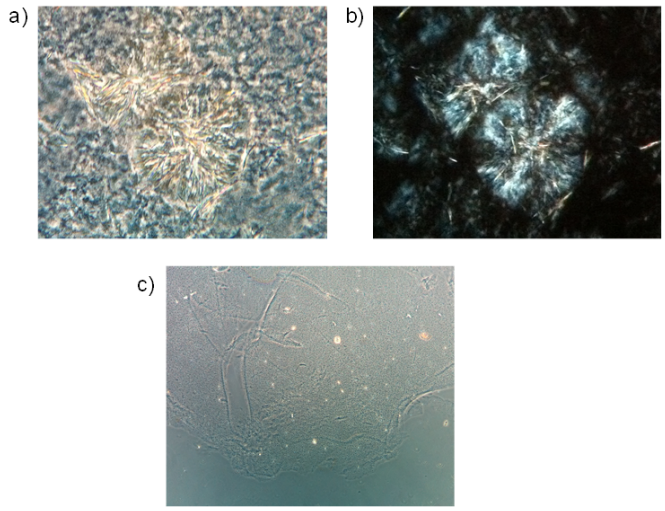

Fig. 6 a) Phase contrast optical image of NPPT gel in toluene b) cross polarized images of NPPT in toluene c) cross polarized optical image of NCT in toluene. The NPPT formed birefringent structures in toluene whereas the NCT gel is non-birefringent (Magnification 20X).

The physical properties of NCT gels were further evaluated by textural profile analysis for large deformations (TPA) (Figure S5). The hardness of NCT gel was found to be 0.68N with high cohesiveness (48.9%) compared to adhesiveness (0.07 N.mm) suggesting that the gel could be self-standing. Attempts to perform TPA on NPPT gel proved futile as they could not generate any textural curve attributed to it's weak viscoelastic nature.

Conclusions

In summary, we shed light onto a rarely explored phenomena which describes significantly strong organogelation behavior attributed to hydrophobic interlocking of *cis* double bonds contributed from a simple amphiphilic system, NCT. The fully saturated control derivative of NCT, i.e., NPPT also results in gelation, however significantly weak in terms of its strength. From SANS, microscopy and simulation studies, we infer that the amphiphiles self-assemble into cylindrical chains of reverse micelles, where the strong gelation ability is attributed to the formation of 3D networks by these chains. Our mesoscale modeling and simulation of NCT in organic solvents proves that additional contribution to significantly high sustainability and mechanical strength of NCT gels stem from the kinked tails of NCT that peg onto each other forming a Velcro like hooking. This in turn strengthen the junctions between the micellar chains which rationalizes the stronger networks formed in case of NCT.

Acknowledgements

This work was in part funded by the following grants to G.J: CBET-1512458 from National Science Foundation (NSF), and GRANT2015-38422-24067 from National Institute of Food and Agriculture (NIFA), United States Department of Agriculture (USDA). One of the authors would like to express her special appreciation and thanks to Scinomics-Maps for their support of the software and advice throughout this project.

Notes and references

[a]Department of Chemistry and Biochemistry and Center for Discovery and Innovation, the City College of New York, 85 St. Nicholas Terrace, New York, NY 10031. E-mail: gjohn@ccny.cuny.edu
[b]Doctoral Program in Chemistry, The City University of New York Graduate Center, 365 5th Avenue, New York, NY 10016
[c]Department of Chemical and Biomolecular Engineering, University of Maryland, College Park, MD 20742. E-mail: sraghava@umd.edu
[d]Department of Mathematics, Central Michigan University, Mount Pleasant, MI 48859. E-mail: leela.rakesh@cmich.edu
[e]Army Research Laboratory, Weapons & Materials Research Directorate, Aberdeen Proving Ground, MD 21005. E-mail: shashi.p.karna.civ@mail.mil
[§]Present address: Advanced Analytical Sciences, Reliance Research & Development Centre, Navi Mumbai 400701, India
[¶] These Authors contributed equally to this work.
†Electronic Supplementary Information (ESI) available: details of computational details rheology and SANS, ^{2}H NMR studies, Optical polarizing microscopic studies, gelation studies, molecular simulations, textural profile analysis, DPD Simulation. See DOI: 10.1039/b000000x/

1. L. B. Smith, T. E. Schäffer, M. Viani, J. B. Thompson, N. A. Frederick, J. Kindt, A. Belcher, G. D. Stucky, D. E. Morse, P.K. Hansma, *Nature* 1995,**399**, 761-763.
2. A. Al-Amoudi, D. Castan˜oDı´ez, M. J. Betts, S. F. Achilleas, *Nature* 2007, **450**, 832-839.
3. H. Lee, B. P Lee, P. B. Messersmith. *Nature* 2007, **448,** 338-341.
4. A. K. Geim, S.V. Dubonos, I.V. Grigorieva, K.S. Novoselov, A.A. Zhukov, S.Y. Shapoval, *Nat. Mater.* **2003**, *2*, 461-463.
5. B. Dragnea *Nat. Mater.* 2008, **7**, 102-104.
6. J. M. Benyus, Biomimicry: Innovation Inspired by Nature. New York, NY: William Morrow and Company, Inc., 1997
7. A. Dejean, C. Leroy, B. Corbara, O. Roux, R. Céréghino, J. Orivel, R. Boulay, *PLoS One* 2010, **5**, 11331-11338.
8. C. Moissl, R. Rachel, A. Briegel, H. Engelhard, R. Huber *Mol. Microbiol*. 2005, **56**, 361–370.
9. H. Ko, J. Lee, B.E. Schubert, Y.L. Chueh, P.W. Leu, R.S. Fearing, A. Javey, *Nano Lett.* 2009,**9**, 2054-2058.
10. P. K. Vemula, G. John, *Acc. Chem. Res.*, 2008,**41**, 769–782.
11. V. S. Balachandran, S. R. Jadhav, P. Pradhan, S. D. Carlo, G. John, *Angew. Chem. Int. Ed.* 2010,**49**, 9509–9512.
12. S. M. Sagnella, C. E. Conn, I. Krodkiewska, X. Mulet, C. J. Drummond, *Soft Matter* 2011, **7**, 5319-5328.
13. G. Lagaly, I. Dékany *Adv. Colloid Interface Sci.* 2005, **114–115,** 189– 204.
14. A. Brizzi, V. Brizzi, M. G. Cascio, T. Bisogno, R. Sirianni, V. Di Marzo, *J. Med. Chem.* 2005, **48**, 7343-7350.
15. M. J. McFarland, A. C. Porter, F. R. Rakhshan, D. S. Rawat, R. A. Gibbs, E. L. Barker, *J. Biol. Chem*. 2004,**279**, 41991–41997.

16. S. M. Sagnella, C. E. Conn, I. Krodkiewska, M. Moghaddam, J. M. Seddon, C. J. Drummond *Langmuir*, 2010, **26**, 3084–3094.
17. J. H. P. Tyman, *Chem. Soc. Rev.* 1979, **8**, 499–537; b) V. S. Balachandran, S. R. Jadhav, P. K. Vemula, G. John, *Chem. Soc. Rev.,* 2013,**42**, 427
18. S.-H. Tung, H.-Y Lee, S. R. Raghavan, *J. Am. Chem. Soc*. 2008, **130,** 8813–8817
19. K. Sun, R. Kumar, D. E. Falvey, S. R. Raghavan, *J. Am. Chem. Soc*., 2009,**131,** 7135–7141.
20. N. M. Correa, J. J. Silber, R. E. Riter and N. E. Levinger, *Chem. Rev*. 2012, **112**, 4569-4602.
21. V. P. Sofía, F. O. Andres and M. P. Gárate, *Current Topics in Med. Chem*. 2014, **14**, 774-780.
22. S. Sarkar, P. Choudhury, S. Dinda, P. K. Das, *Langmuir*, 2018, **34**, 10449-10468.
23. R. Urano, G. A. Pantelopulos, J. E. Straub, *J. Phys. Chem. B*. 2019, **123**, 2546-2557.
24. D. Singha, D. K. Sahu, K. Sahu, *J. Phys. Chem. B*. 2018, **122**, 6966-6974.
25. D. Blach, M. Pessêgo, J. J. Silber, N. M. Correa, L. García-Río, R. D. Falcone, *Langmuir*, 2014, **30**, 12130-12137.
26. A. Kakgo, S. Sugimoto, J. P. Gong, Y. Osada, *Adv. Mater*., 2002,**14,** 1124-1126.
27. S. Zhang, M. A. Greenfield, A. Mata, L. C. Palmer, R. Bitton, J. R. Mantei, C. Aparicio, M. O. de la Cruz, S. I. Stupp, *Nat. Mater.* 2010**, 9,** 594-601.
28. P. Lenz, D. R. Nelson, *Phys. Rev. E,* 2003,**67**, 031502 1-19.
29. E. Moeendarbary, T. Y. Ng, M. Zangeneh, *Int. J. Appl. Mechanics*. 2009, **1**, 737-763.
30. B. Luy, K. Kobzar, H. Kessler, *Angew. Chem. Int. Ed.* 2004,**43**, 1092 -1094.
31. W.K. den Otter, S. A. Shkulipa, *Biophys. J.* 2007, **93**, 423-433.
32. A. Galuschko, L. Spirin, T. Kreer, A. Johner, C. Pastorino, J. Wittmer, J. Baschnagel, *Langmuir* 2010, **26,** 6418-6429.
33. J. Klein. Y. Kamiyama, H. Yoshizawa, J. N. Israelachvili, G. Fredrickson, P. Pincus, L. J. Fetters, M*acromolecules* 1993, **26,** 5552-5560.
34. W. Rawicz, K.C. Olbrich, T. McIntosh, D. Needham, E. Evans, *Biophys. J,* 2000, **79,** 328-339.
35. G. John, J. H. Jung, M. Masuda, T. Shimizu, *Langmuir* 2004, **20**, 2060-2065.
36. R. M. Pashley, M. E. Karaman*, Applied Colloid & Surface Chemistry, p. 69, Wiley-2004, NY USA*

Gelation of amphiphiles due to the formation of networks of cylindrical chains of reverse micelles is observed.